

# Confinement of graphene Dirac fermions in electric and magnetic fields with displacement symmetry in one direction

İsmail Burak Ateş<sup>a\*</sup>, Şengül Kuru<sup>a†</sup>, Javier Negro<sup>b‡</sup>

<sup>a</sup>Department of Physics, Faculty of Science, Ankara University, 06100 Ankara, Turkey

<sup>b</sup>Departamento de Física Teórica, Atómica y Óptica, Universidad de Valladolid, 47071 Valladolid, Spain

July 26, 2022

## Abstract

In this paper, analytical solutions of the Dirac-Weyl equation in the presence of electric and magnetic fields are discussed for low energy electrons in graphene. In order to obtain analytical expressions we have made use of a displacement symmetry of the system along a direction. Simple conditions on magnetic and electric fields have been obtained in order to apply our results based on supersymmetric quantum mechanics methods. The example of an electric well is worked out in detail to illustrate some of the most interesting features of this procedure.

## 1 Introduction

Graphene being the first example of two-dimensional crystals has attracted much attention in physics due to its important electronic and optical properties [1, 2, 3]. The dynamics of low-energy, massless spin 1/2 Dirac electrons with Fermi-velocity in graphene is described by the (2+1) dimensional Dirac-Weyl equation [2]. The analytical solutions of this equation in the presence of different external magnetic and electric fields and the interpretation of its results, has brought great interest in recent years for its applications to graphene and other allotropes of carbon. For instance, it is essential for a better knowledge of the electronic properties of nanoribbons, nanowires and nanotubes. In particular, studies on graphene quantum dots, graphene nanostrips, also known as artificial atoms, contribute to basic physics, electronics, optics, etc. which have numerous applications [4, 5, 6]. Therefore, not only theoretical but also experimental studies are conducted to understand the confinement mechanism of Dirac electrons in graphene [7, 8]. Due to Klein tunnelling, it is known the difficulty to trap Dirac electrons in graphene by means of electrostatic potential [1, 9, 10]; it is much easier to confine them by means of magnetic fields [11, 12, 13, 14, 15, 16, 17, 18, 19]. However, since electrostatic potential may be more advantageous in practice, many studies on electric confinement have also been carried out recently [20, 21, 22, 23, 24, 25, 26, 27]. Remark that electric fields acting on a graphene sheet, may produce a pseudomagnetic field by uniaxial strain [27, 28, 29, 30] which is important in engineering due to their effects on the spectrum.

The aim of this study is to search for analytical methods to obtain solutions, or approximations, to the

\*ismailburakates@gmail.com, ORCID: [0000-0001-8262-2572](https://orcid.org/0000-0001-8262-2572)

†sengul.kuru@science.ankara.edu.tr, ORCID: [0000-0001-6380-280X](https://orcid.org/0000-0001-6380-280X)

‡jnegro@uva.es, ORCID: [0000-0002-0847-6420](https://orcid.org/0000-0002-0847-6420)

trapping mechanisms of Dirac electrons in graphene under magnetic and electric external fields. In the present work we will restrict to systems with displacement symmetry along one direction (the  $y$  axis) to facilitate the approach. The different conditions that we will find to classify these systems can be applied to many results scattered in the recent literature. Thus, we wish they to be considered under the same point of view which consist in three options: pure magnetic or electric field, or both mixed perpendicular electric and magnetic fields. We will deal in detail with one example of pure electric field in order to show some not so well known peculiarities: the role of the symmetry momentum  $k_y$  in this problem; the electric potential as an effective complex potential; the supersymmetric character of effective complex potentials.

Supersymmetric quantum mechanics has been shown to be a very fruitful tool for finding and analyzing exact solutions to some 1-dimensional problems [31]. This method can also be applied to the 2D Dirac-Weyl equation [12, 13, 14, 15, 27, 31, 33, 35]. Within the scope of this work, it is aimed to find and solve the problems involving electric and/or magnetic fields by means of this method. This requires a specific form of electric and magnetic fields in a certain way; therefore, it is often difficult that these fields be relevant in experimental studies. However, such problems are theoretically important and can contribute to a more comfortable understanding of some of the facts encountered in practice.

The organization of the paper is as follows. In Section 2 we present the general set up of the Dirac-Weyl equation interacting with electric and magnetic fields. A matrix  $M$  is introduced which determine the three possible cases. These cases are analysed in Section 3; they correspond to pure magnetic or electric fields and both fields together. The pure electric field is carefully examined through an example. The last section enumerates the most interesting results of the work.

## 2 Interactions with symmetry in the $y$ -axis direction

We will consider the stationary Dirac-Weyl equation for quasi-particles of zero mass and  $1/2$  spin but with the charge of an electron. This is the way to describe the electronic interaction in graphene for a range of energies near to the Dirac points (hereafter we will restrict to one of them,  $K$ ). The equation for the interaction in external fields, applying the minimal coupling rule, is

$$v_F(\boldsymbol{\sigma} \cdot (\mathbf{p} + e\mathbf{A}))\Psi(\mathbf{x}) = (E - V(\mathbf{x}))\Psi(\mathbf{x}) \quad (2.1)$$

where, as usual  $\boldsymbol{\sigma} = (\sigma_x, \sigma_y)$  are sigma Pauli matrices,  $\mathbf{p}$  the two-component momentum operator in the  $xy$ -plane,  $v_F$  the Fermi velocity of graphene,  $e$  the electric charge and  $\mathbf{A}(\mathbf{x})$ ,  $V(\mathbf{x})$  magnetic and electric potentials defined on the plane.

We will assume the symmetry of the fields along displacements in one direction (in the  $y$ -direction) and both fields to be perpendicular (the electric one on the  $xy$ -plane, the magnetic in the  $z$ -direction perpendicular to the graphene plane). In fact, we will restrict to the potentials having the form

$$\mathbf{A}(\mathbf{x}) = (0, A_y(x)), \quad V(\mathbf{x}) = V(x) \quad (2.2)$$

Therefore, the magnetic field may depend only on  $x$  in this case and it is given by  $\mathbf{B}(x) = A'_y(x)\hat{z} = \frac{dA_y(x)}{dx}\hat{z}$ , where  $\hat{z}$  is the unit vector of  $z$ -axis; while the electric field  $\mathbf{E}(x) = -V'(x)\hat{x} = \frac{dV(x)}{dx}\hat{x}$  will have the  $x$ -direction and it may depend also on  $x$ . Hereafter, the ‘‘prime’’, will be used for derivatives with respect to the argument. Then, we can choose the wavefunction of (2.1) to be an eigenfunction of the translation operator  $p_y = -i\hbar\partial_y$ , with eigenvalue  $\hbar k$ ,

$$\Psi(x, y) = e^{iky} \begin{pmatrix} \psi_1(x) \\ i\psi_2(x) \end{pmatrix}, \quad p_y\Psi(x, y) = \hbar k\Psi(x, y) \quad (2.3)$$

where the imaginary unit  $i$  has been included in the second component by convenience. Replacing these fields and operators together in the initial equation (2.1), we have

$$\hbar v_F \begin{pmatrix} 0 & \partial_x + k + e/\hbar A_y(x) \\ -\partial_x + k + e/\hbar A_y(x) & 0 \end{pmatrix} \begin{pmatrix} \psi_1(x) \\ \psi_2(x) \end{pmatrix} = (E - V(x)) \begin{pmatrix} \psi_1(x) \\ \psi_2(x) \end{pmatrix} \quad (2.4)$$

This equation can be considered as a matrix differential eigenvalue problem, where the energy  $E$  plays the role of eigenvalue while the matrix differential operator has a Hermitian character on an appropriate space. Our aim here is just to compute the solution in some cases.

Next, we will manipulate this equation to see if it can be diagonalized (or decoupled). Thus, the equation can also be rewritten in the following form

$$\begin{pmatrix} \partial_x & 0 \\ 0 & \partial_x \end{pmatrix} \begin{pmatrix} \psi_1(x) \\ \psi_2(x) \end{pmatrix} = \begin{pmatrix} (k + \frac{e}{\hbar} A_y(x)) & -(E - V(x))/\hbar v_F \\ (E - V(x))/\hbar v_F & -(k + \frac{e}{\hbar} A_y(x)) \end{pmatrix} \begin{pmatrix} \psi_1(x) \\ \psi_2(x) \end{pmatrix} \quad (2.5)$$

We can simplify the notation as follows:

$$W(x) := k + e/\hbar A_y(x) := k + \mathcal{A}_y(x), \quad \Delta(x) := \frac{E}{\hbar v_F} - \frac{V(x)}{\hbar v_F} := \varepsilon - \mathcal{V}(x), \quad (2.6)$$

so that  $W(x)$  is related to the magnetic potential and  $\Delta(x)$  with the electric one. Finally, we have obtained the Dirac-Weyl equation as a linear normal system of two equations (in other words, with only the derivative of the components to the left):

$$\partial_x \Psi_R(x) = M \Psi_R(x) \quad (2.7)$$

where the  $M$  matrix and the column vector  $\Psi_R(x)$  are

$$M = \begin{pmatrix} W(x) & -\Delta(x) \\ \Delta(x) & -W(x) \end{pmatrix}, \quad \Psi_R(x) = \begin{pmatrix} \psi_1(x) \\ \psi_2(x) \end{pmatrix} \quad (2.8)$$

Notice that this system of two linear equations is real and we are looking for real square integrable solutions  $\Psi_R(x) = \Psi_R(x)^*$ ,

$$\psi_1(x) = \psi_1(x)^*, \quad \psi_2(x) = \psi_2(x)^*$$

Differentiating equation (2.7) gives

$$\partial_{xx} \Psi_R(x) = (M' + M^2) \Psi_R(x) \quad (2.9)$$

where  $M^2$  is diagonal, while  $M' = \frac{dM(x)}{dx}$  carries the nondiagonal part:

$$M'(x) = \begin{pmatrix} W'(x) & -\Delta'(x) \\ \Delta'(x) & -W'(x) \end{pmatrix}, \quad M^2 = (W(x)^2 - \Delta(x)^2) I \quad (2.10)$$

In order to diagonalize  $M'(x)$ , first we take its square:

$$M'(x)^2 = (W'(x)^2 - \Delta'(x)^2) I$$

Therefore, the two eigenvalues of  $M'(x)$  should be

$$\lambda_{\pm} = \pm \sqrt{W'(x)^2 - \Delta'(x)^2} = \pm \sqrt{\mathcal{A}'_y{}^2 - \mathcal{V}'^2}$$

In the following we will discuss the simplest options.

### 3 Solvable cases

In this formulation of the problem, we must diagonalize  $M' \rightarrow D = T^{-1}M'T$  by means of a constant matrix,  $T$ , in order that it should commute with the differential operator  $\partial_{xx}$  in equation (2.9). There are three situations where this is possible, as it will be seen below.

#### 3.1 Pure magnetic field $\mathcal{V} = 0$

In this first case,  $\Delta'(x) = \mathcal{V}'(x) = 0$ , that is, we have a pure magnetic field.

$$M'(x) = \begin{pmatrix} W'(x) & 0 \\ 0 & -W'(x) \end{pmatrix}, \quad M^2 = (W(x)^2 - \varepsilon^2) I$$

This is the simplest case, where we have only a magnetic field perpendicular to the plane  $XY$ , determined by the component  $\mathcal{A}_y$ . Besides, the matrix  $M'(x)$  is already diagonal, and equation (2.9) shows the supersymmetric form of the problem:

$$\begin{pmatrix} -\partial_{xx} + W'(x) + W(x)^2 & 0 \\ 0 & -\partial_{xx} - W'(x) + W(x)^2 \end{pmatrix} \Psi_R(x) = \varepsilon^2 \Psi_R(x) \quad (3.11)$$

where  $W(x)$  plays the role of superpotential. This case was exhaustively studied in previous references [3, 11, 12, 13, 14, 15, 16, 33].

#### 3.2 Pure electric field $\mathcal{A}(x) = 0$

In this case equation (2.9) takes the form

$$\partial_{xx} \Psi_R(x) = \Delta'(x) \begin{pmatrix} 0 & -1 \\ 1 & 0 \end{pmatrix} \Psi_R(x) + (k^2 - \Delta(x)^2) \begin{pmatrix} 1 & 0 \\ 0 & 1 \end{pmatrix} \Psi_R(x) \quad (3.12)$$

where the non-diagonal matrix is

$$M'(x) = \Delta'(x) \begin{pmatrix} 0 & -1 \\ 1 & 0 \end{pmatrix} = \mathcal{V}'(x) \begin{pmatrix} 0 & 1 \\ -1 & 0 \end{pmatrix}$$

In this case the eigenvalues are complex and the matrix  $M'$  can be diagonalized into  $\tilde{M}'$  with the help of a complex matrix  $T$ :

$$\tilde{M}' = T^{-1}M'T = \begin{pmatrix} -i\mathcal{V}'(x) & 0 \\ 0 & i\mathcal{V}'(x) \end{pmatrix}, \quad T = \begin{pmatrix} 1 & 1 \\ i & -i \end{pmatrix}, \quad T^{-1} = \frac{1}{2i} \begin{pmatrix} i & 1 \\ i & -1 \end{pmatrix}$$

Then, defining

$$\tilde{\Psi} = T^{-1}\Psi_R \implies \begin{cases} \tilde{\psi}_1 = \frac{1}{2}(\psi_1 - i\psi_2) \\ \tilde{\psi}_2 = \frac{1}{2}(\psi_1 + i\psi_2) \end{cases} \quad (3.13)$$

the system of equations (3.12) becomes

$$\partial_{xx} \tilde{\Psi}(x) = (\tilde{M}'(x) + \tilde{M}^2) \tilde{\Psi}(x) \quad (3.14)$$

which consists in two complex conjugate equations, one for each component:

$$\begin{cases} \left( -\partial_{xx} + V_1(x) \right) \tilde{\psi}_1 := \left( -\partial_{xx} - (i\Delta)' + (i\Delta)^2 \right) \tilde{\psi}_1 = -k^2 \tilde{\psi}_1 \\ \left( -\partial_{xx} + V_2(x) \right) \tilde{\psi}_2 := \left( -\partial_{xx} + (i\Delta)' + (i\Delta)^2 \right) \tilde{\psi}_2 = -k^2 \tilde{\psi}_2 \end{cases} \quad (3.15)$$

Let us mention some aspects of the above equations.

1. If  $\tilde{\psi}_1$  is a solution of the first equation, then its complex conjugate  $\tilde{\psi}_1^* := \tilde{\psi}_2$  will be a solution of the second.
2. Each of the two equations may have a PT symmetric Hamiltonian  $V_i(x) = V_i(-x)^*$  [36, 37, 38]. For example, if the potential  $\mathcal{V}$  is even and therefore  $V_i$ ,  $i = 1, 2$  are also even. The question is if the PT symmetry is broken or not.
3. The equations have potentials depending on the energy of the initial Dirac-Weyl problem. In this case the role of  $k$  and  $\varepsilon$  has been interchanged with respect to the pure magnetic case in (2.4). However, we assume that  $k$  is a continuous parameter and for each value of  $k$  we should have a discrete number of energies  $\varepsilon_n(k)$ .
4. We will have complex solutions, but the spectrum given by the eigenvalues  $\varepsilon$  must be real. The Dirac-Weyl equation (2.7) in the new components is obtained by applying  $T^{-1}$  of (3.13). The resulting pair of equations take the form

$$\begin{cases} (\partial_x + i\Delta(x))\tilde{\psi}_1(x) = k\tilde{\psi}_2 \\ (\partial_x - i\Delta(x))\tilde{\psi}_2(x) = k\tilde{\psi}_1 \end{cases}, \quad \Delta(x) = \varepsilon - \mathcal{V}(x) \quad (3.16)$$

Therefore, the solutions must satisfy the separated equations (3.15) and also the Dirac-Weyl equations (3.16). As we will see later, in an example, the solutions of (3.15) can be chosen conjugate, but one must find the right complex phase coefficient so that the coupled equations (3.16) be also satisfied.

5. Remark that eq. (3.16) together with (3.15) have the characteristic form of SUSY-qm, where the intertwining operators  $A^\pm$  have complex superpotentials,  $A^\pm = \partial_x \pm i\Delta(x)$ .

We can apply this formalism to different electric potentials. We have to take into account the asymptotic conditions of the potential  $\mathcal{V}(x)$  in order the Schrödinger like equations (3.15) have square-integrable eigenfunctions corresponding to a discrete spectrum. Take, for instance the first equation of (3.15) and rewrite it as follows:

$$\left( -\partial_{xx} + (-i\mathcal{V}' + 2\varepsilon\mathcal{V} - \mathcal{V}^2) \right) \tilde{\psi}_1 = -(k^2 - \varepsilon^2) \tilde{\psi}_1 \quad (3.17)$$

We consider an effective complex potential (depending on  $\varepsilon$ )

$$V_{\text{eff}}(x) = i\mathcal{V}' + 2\varepsilon\mathcal{V} - \mathcal{V}^2 \quad (3.18)$$

and an effective energy

$$E_{\text{eff}} = -(k^2 - \varepsilon^2) \quad (3.19)$$

Let us assume, for instance, that  $V_{\text{eff}}(x)^\pm \rightarrow 0$  when  $x \rightarrow \pm\infty$ . Then, a necessary condition to have an square integrable eigenfunction is, according to (3.19), that  $|\varepsilon| < |k|$ ; in other words, in the context

of null mass graphene quasiparticle, the parallel momentum  $k$  plays a similar role of the mass in a Dirac particle. We will see in the following example a simple case to confirm this behaviour.

In general, the conditions to have an effective well potential are not easy to satisfy if we are interested in potentials allowing for analytic solutions. Some examples considered in previous references are the following. a)  $\mathcal{V}(x) = \frac{e}{|x|}$ , similar to the Coulomb potential but in one dimension [24]; b)  $\mathcal{V}(x) = \frac{e}{1+x^2}$ , a Lorentzian type potential [24]; c)  $\mathcal{V}(x) = \tanh x$ , a Pöschl-Teller like potential [25].

A way to obtain partly analytic formulas of eigenfunctions is to make use of piecewise regular functions for the potentials and then apply matching conditions. This is the case of the following example that we will work out in detail. It will give us the main features of the discrete spectrum and a number of properties of the electric interaction: Boundary lines of the spectrum; atomic collapses produced by deepening the potential; the role of the parallel momentum  $k$ , or the shape and orthogonality of the complex eigenfunctions.

### 3.3 Square well potential

Let the square potential be defined by

$$\mathcal{V}(x) = \begin{cases} -v_0, & |x| < 1, \\ 0, & |x| > 1 \end{cases} \quad (3.20)$$

The corresponding Schrödinger equation with effective potential (3.18) is:

$$-\tilde{\psi}_1''(x) + V_{\text{eff}}(x) = -(k^2 - \varepsilon^2)\tilde{\psi}_1 \quad (3.21)$$

Here the effective potential is complex and has the following form:

$$V_{\text{eff}}(x) = \begin{cases} -iv_0\delta(x+1) + iv_0\delta(x-1) - 2v_0\varepsilon - v_0^2, & |x| \leq 1, \\ 0, & |x| > 1 \end{cases} \quad (3.22)$$

For this potential we have three different regions:  $x < -1$ ,  $-1 < x < 1$ , and  $x > 1$ . In the first and third region the potential vanishes while, in the second one is a constant  $(-2v_0\varepsilon - v_0^2)$ . Each region is separated from its neighbour by a Dirac's delta with imaginary intensity. Next, we write the solutions corresponding to bound states within each of these regions:

- $x < -1$ :

$$\begin{aligned} -\tilde{\psi}_{1,I}''(x) &= -p^2\tilde{\psi}_{1,I}, & p^2 &= k^2 - \varepsilon^2 > 0 \\ \tilde{\psi}_{1,I}(x) &= Ae^{px}, & p &= \sqrt{k^2 - \varepsilon^2} > 0 \end{aligned} \quad (3.23)$$

- $-1 < x < 1$ :

$$\begin{aligned} -\tilde{\psi}_{1,II}''(x) + (-2v_0\varepsilon - v_0^2)\tilde{\psi}_{1,II} &= -p^2\tilde{\psi}_{1,II}, & q^2 &= 2v_0\varepsilon + v_0^2 - p^2 > 0 \\ \tilde{\psi}_{1,II}(x) &= Ce^{iqx} + De^{-iqx}, & q &= \sqrt{(\varepsilon + v_0)^2 - k^2} > 0 \end{aligned} \quad (3.24)$$

- $x > 1$ :

$$\begin{aligned} -\tilde{\psi}_{1,III}''(x) &= -p^2\tilde{\psi}_{1,III}, & p^2 &= k^2 - \varepsilon^2 > 0 \\ \tilde{\psi}_{1,III}(x) &= Fe^{-px}, & p &= \sqrt{k^2 - \varepsilon^2} > 0 \end{aligned} \quad (3.25)$$

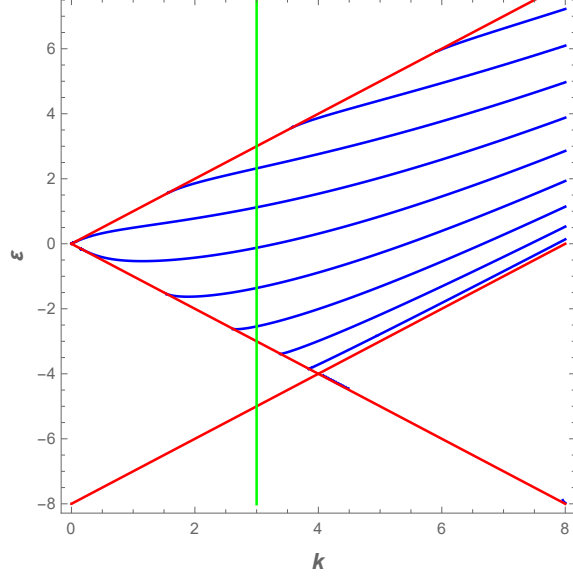


Figure 1: The energy eigenvalues for a fixed value  $v_0$  are limited by  $|\varepsilon| < k$  (3.23) and by  $|\varepsilon + v| > k$  (3.24). In this case the energy levels are for  $v_0 = 8$ ,  $k > 0$ .

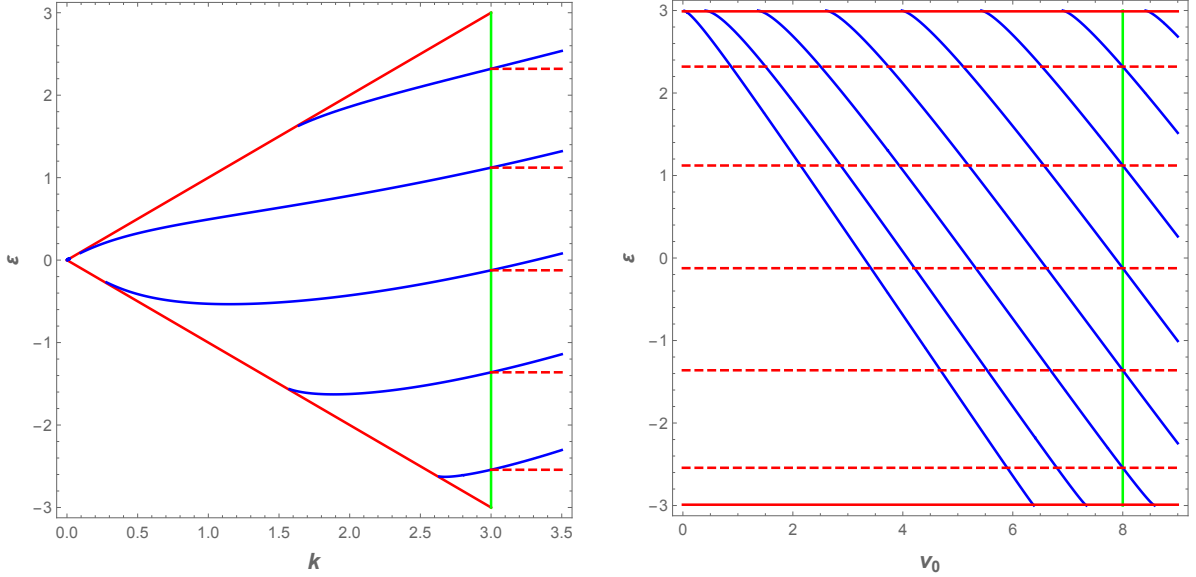


Figure 2: (left) Graphic of energy eigenvalues as a function of  $k$  for a fixed value  $v_0 = 8$  and the border lines  $\varepsilon = \pm k$  (the green vertical line is for  $k = 3$ ). (right) Graphic of energy  $\varepsilon$  versus the depth  $v_0$  of the well for  $k = 3$ . The green line corresponds to  $v_0 = 8$ ; the spectrum of the two vertical green lines should coincide (as shown by the dashed red lines).

These solutions satisfy continuity conditions at  $x = -1$  and  $x = 1$ .

$$\begin{aligned}
 \tilde{\psi}_{1,I}(-1) &= \tilde{\psi}_{1,II}(-1), & \tilde{\psi}'_{1,I}(-1) &= \tilde{\psi}'_{1,II}(-1) + iv_0\tilde{\psi}_{1,I}(-1) \\
 \tilde{\psi}_{1,II}(1) &= \tilde{\psi}_{1,III}(1), & \tilde{\psi}'_{1,II}(1) &= \tilde{\psi}'_{1,III}(1) - iv_0\tilde{\psi}_{1,II}(1)
 \end{aligned}
 \tag{3.26}$$

From these conditions we have four equations for  $A, C, D, F$ :

$$\begin{aligned}
Ae^{-p} - Ce^{-iq} - De^{iq} &= 0 \\
A(pe^{-p} - iv_0e^{-p}) - C(iq)e^{-iq} + D(iq)e^{iq} &= 0 \\
Ce^{iq} + De^{-iq} - Fe^{-p} &= 0 \\
C(iq)e^{iq} + D(-iq)e^{-iq} + F(pe^{-p} + iv_0e^{-p}) &= 0
\end{aligned} \tag{3.27}$$

This is a homogeneous system for the unknown parameters  $A, C, D, F$ . The solutions exist when the determinant of the coefficients vanishes. Then, we get the relation between  $\varepsilon, k$  and  $v_0$ :

$$\left( \sqrt{k^2 - \varepsilon^2} \sqrt{(\varepsilon + v_0)^2 - k^2} \cos \left( 2\sqrt{(\varepsilon + v_0)^2 - k^2} \right) - (\varepsilon(\varepsilon + v_0) - k^2) \sin \left( 2\sqrt{(\varepsilon + v_0)^2 - k^2} \right) \right) = 0$$

Fig. 1 shows the graphic of  $\text{Im}(\det M) = 0$  for a range of  $k$  and  $\varepsilon$  once fixed  $v_0 = 8$ . The curves in blue represent the values of the energy. Lines  $\varepsilon = \pm k$  determine the domain where the solutions may exist. In particular, the solutions on  $\varepsilon = \pm k$  correspond to the critical values for the bound state energies. Another boundary line is given by  $\varepsilon + v_0 = k$  according to (3.24). Therefore, only when  $\varepsilon + v_0 > k$  and  $\varepsilon < k$  are satisfied, there will be solutions of the previous equations. These inequalities can be seen in Fig. 1 by means of red lines.

It is quite significant the plot of the  $\varepsilon$  dependence of the potential  $v_0$  for fixed values of  $k$  where the collapses of negative bound states in the negative sea can be appreciated [39, 40]. This is shown in the plot to the right of Fig. 2 of the spectrum corresponding to  $v_0 = 8$ . In this case the lowest state of the spectrum it is not a fundamental state due to two previous colapses, so that in fact, this is the second excited state.

Fig. 3 is similar to Fig. 2, but in this case  $v_0 = 2$  for the left graphic, while  $k = 2$  for the right one (as can be seen, there is no collapses). The states of the three points of the spectrum determined by the green lines have been obtained and plotted in Figs. 4-6. It is quite interesting the information of these complex eigenfunctions: i) For each spinor the two components are complex conjugate of each other:  $\tilde{\psi}_1(x) = \tilde{\psi}_2(x)^*$ . ii) The solutions  $\tilde{\Psi}$  corresponding to different energy levels are orthogonal and therefore also the spinors  $\tilde{\Psi}$  are orthogonal. The orthogonality is defined as follows. Let  $\tilde{\Psi}^a = (\tilde{\psi}_1^a, \tilde{\psi}_2^a)$  the spinor components of an state  $\tilde{\Psi}^a$  with energy  $E^a$ , and  $\tilde{\Psi}^b$  that one with energy  $E^b \neq E^a$ . Then, the orthogonality is defined by

$$\langle \tilde{\Psi}^a, \tilde{\Psi}^b \rangle = \int_{-\infty}^{\infty} (\tilde{\psi}_2^a \tilde{\psi}_1^b + \tilde{\psi}_1^a \tilde{\psi}_2^b) dx = \frac{1}{2} \int_{-\infty}^{\infty} (\psi_1^a \psi_1^b + \psi_2^a \psi_2^b) dx = 0$$

iii) Remark that  $\tilde{\psi}_1$  and  $\tilde{\psi}_2$  not only satisfy (3.15) and complex conjugate each other but also they satisfy the equations (3.16). So, it may be necessary to multiply  $\tilde{\psi}_1$  and  $\tilde{\psi}_2$  by conjugate phases. The graphics of spinor elements of wave functions ( $\tilde{\psi}_i(x), i = 1, 2$ ) are plotted in Figs. 4-6. From these graphics it can be seen that these solutions have  $PT$  symmetry. In other words, the energy eigenfunctions  $\tilde{\psi}_k(x)$  are also eigenfunctions of the  $PT$  operator (made of complex conjugation  $T$  and  $x$  parity  $P$ ) with eigenvalues  $\pm i$ :

$$PT\tilde{\psi}_k(x) := \tilde{\psi}_k(-x)^* = (\pm i)\tilde{\psi}_k(x), \quad k = 1, 2$$

Using  $\tilde{\psi}_{1,2}$ , the solutions of Dirac Weyl equation given by (2.3) can be obtained. In order to do this, first we use equation (3.13) to get  $\psi_{1,2}$  in terms of  $\tilde{\psi}_{1,2}$ . Thus, the spinor solutions of Dirac-Weyl equation are:



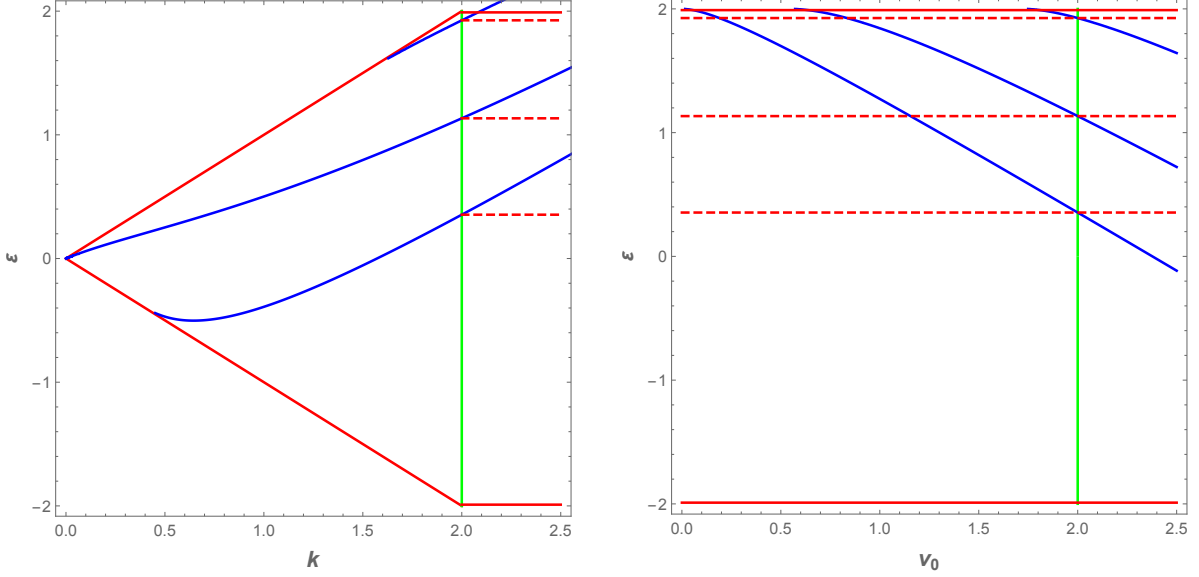


Figure 3: (left) Graphic of  $\text{Im}(\det M) = 0$  (energy eigenvalues) for a fixed value  $v_0 = 2$  and the border lines  $\varepsilon = \pm k$ ; and (right) the graphic of energy  $\varepsilon$  versus the depth  $v_0$  of the well for  $k = 2$ .

$$\Psi_n(x, y) = 2e^{iky} \begin{pmatrix} \text{Re}\tilde{\psi}_{1n}(x) \\ -\text{Im}\tilde{\psi}_{1n}(x) \end{pmatrix} \quad (3.28)$$

Then, probability density

$$\rho_n = |\Psi_n(x, y)|^2 = 4((\text{Re}\tilde{\psi}_{1n}(x))^2 + (\text{Im}\tilde{\psi}_{1n}(x))^2) \quad (3.29)$$

and current density

$$J_{nx} = \Psi_n^\dagger(x, y)\sigma_x\Psi_n(x, y) = -8(\text{Re}\tilde{\psi}_{1n}(x))(\text{Im}\tilde{\psi}_{1n}(x)), \quad J_{ny} = \Psi_n^\dagger(x, y)\sigma_y\Psi_n(x, y) = 0 \quad (3.30)$$

are found. The graphics of them for fixed values of  $k$  and  $v$  can be seen in Fig. 7.

### 3.4 Proportional electromagnetic fields: $\mathcal{V} \propto \mathcal{A}$

In this case we will assume that both potential intensities have proportional form,

$$\mathcal{V}(x) = \alpha\mathcal{A}(x) \implies \begin{cases} W(x) = k + \mathcal{A}(x) \\ \Delta(x) = \alpha(\tilde{\varepsilon} - \mathcal{A}(x)) \end{cases}$$

where we have introduced  $\varepsilon = \alpha\tilde{\varepsilon}$ . Then, we can write

$$\Delta'(x) = -\alpha\mathcal{A}'(x), \quad W'(x) = \mathcal{A}'(x)$$

Thus, the matrices  $M'$  and  $M^2$  will take the form

$$M'(x) = \mathcal{A}'(x) \begin{pmatrix} 1 & \alpha \\ -\alpha & -1 \end{pmatrix} := \mathcal{A}'(x)M_\alpha, \quad M^2 = \left( (k + \mathcal{A}(x))^2 - (\varepsilon - \alpha\mathcal{A}(x))^2 \right) I$$

We can have the following possibilities:

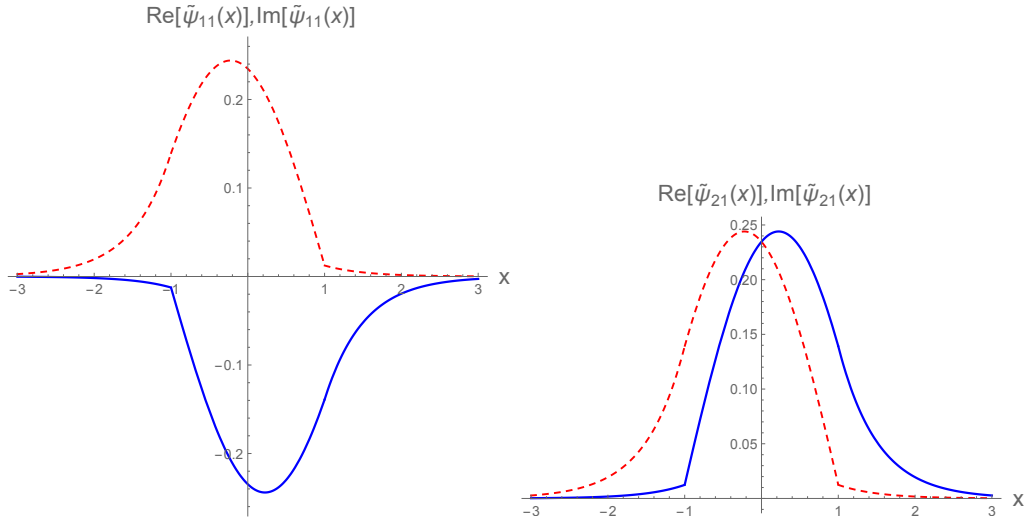


Figure 4: The graphic of real part (dotted) and imaginary part (continuous) of the solution  $\tilde{\psi}_{11}(x)$  and  $\tilde{\psi}_{21}(x)$  for  $v_0 = 2$ ,  $k = 2$  and  $\varepsilon_1 = 0.354274$ .

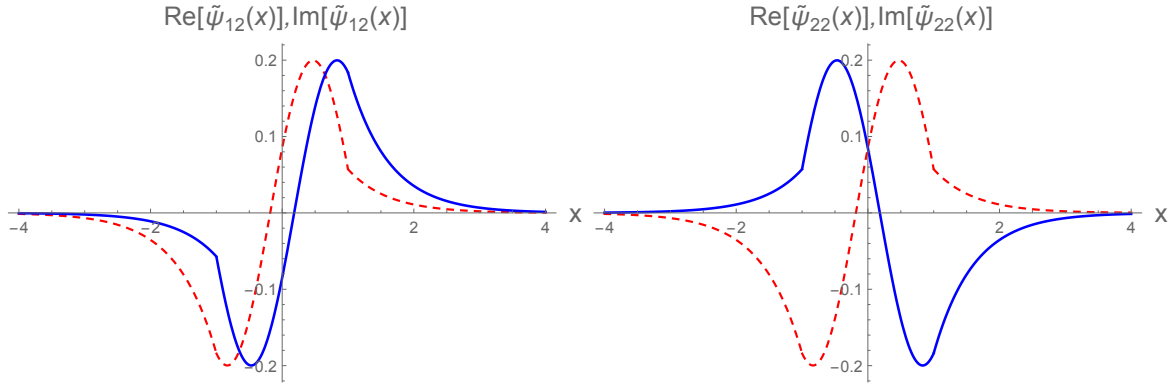


Figure 5: The graphic of real part (dotted) and imaginary part (continuous) of the solution  $\tilde{\psi}_{12}(x)$  and  $\tilde{\psi}_{22}(x)$  for  $v_0 = 2$ ,  $k = 2$  and  $\varepsilon_2 = 1.13356$ .

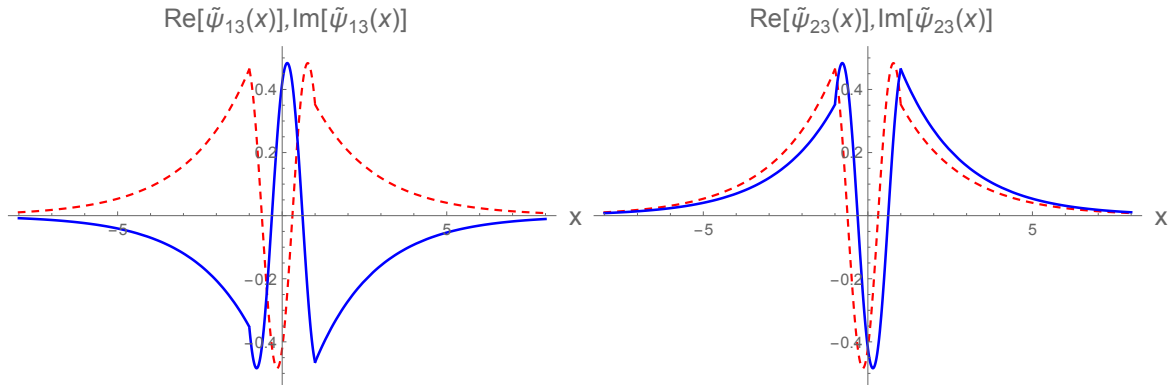


Figure 6: The graphic of real part (dotted) and imaginary part (continuous) of the solution  $\tilde{\psi}_{13}(x)$  and  $\tilde{\psi}_{23}(x)$  for  $v_0 = 2$ ,  $k = 2$  and  $\varepsilon_3 = 1.92583$ .

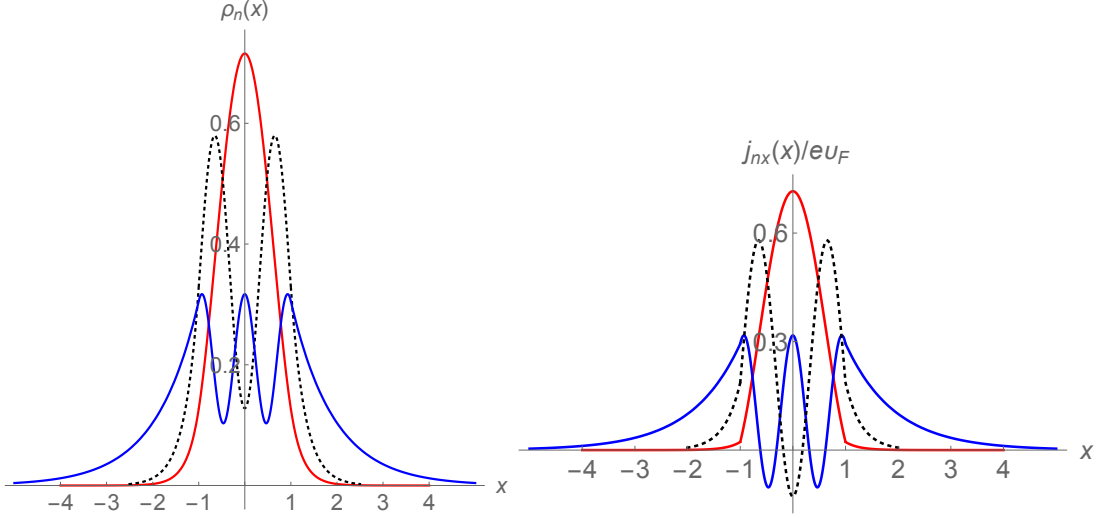


Figure 7: The graphic of probability and current densities for  $v_0 = 2$ ,  $k = 2$  and  $\varepsilon_3 = -2.54$ .

- a)  $|\alpha| < 1$  (trigonometric or  $\mathcal{A}$ -dominant)
- b)  $|\alpha| > 1$  (hyperbolic or  $\mathcal{V}$ -dominant)
- c)  $\alpha = \pm 1$ , (parabolic or equal  $\mathcal{A}$ - $\mathcal{V}$ )

Henceforth we will assume  $0 < |\alpha| < 1$ . The second order equation (2.9) can be written in the form

$$-\Psi_R''(x) + \left( \mathcal{A}'(x)M_\alpha + \left( (k + \mathcal{A}(x))^2 - (\varepsilon - \alpha\mathcal{A}(x))^2 \right) I \right) \Psi_R(x) = 0 \quad (3.31)$$

Next, we diagonalize the matrix  $M_\alpha$  by means of the eigenvalues and eigenvectors:

$$\lambda_\pm = \pm\sqrt{1 - \alpha^2}, \quad \mathbf{v}_\pm = \begin{pmatrix} \alpha \\ -1 \pm \sqrt{1 - \alpha^2} \end{pmatrix}$$

Sometimes we use the notation  $\alpha = \sin \gamma$ ; in this case we have

$$\lambda_\pm = \pm \cos \gamma, \quad \mathbf{v}_\pm = \begin{pmatrix} \sin \gamma \\ -1 \pm \cos \gamma \end{pmatrix}$$

The diagonalization is realized by means of the matrix  $S$  as follows,

$$\Psi_R(x) = S\Psi_D(x), \quad D_\alpha = S^{-1}M_\alpha S = \begin{pmatrix} \sqrt{1 - \alpha^2} & 0 \\ 0 & -\sqrt{1 - \alpha^2} \end{pmatrix}, \quad S = \begin{pmatrix} \alpha & \alpha \\ -1 + \sqrt{1 - \alpha^2} & -1 - \sqrt{1 - \alpha^2} \end{pmatrix}$$

Once replaced these expressions in (3.31) we get

$$-\Psi_D''(x) + \left( \mathcal{A}'(x)D_\alpha + \left( \frac{\varepsilon\alpha + k}{\sqrt{1 - \alpha^2}} + \sqrt{1 - \alpha^2}\mathcal{A}(x) \right)^2 - \frac{(\varepsilon + \alpha k)^2}{1 - \alpha^2} I \right) \Psi_D(x) = 0 \quad (3.32)$$

Let us call the (upper and lower) components of  $\Psi_D(x)$  in the form  $\psi_D^+(x)$  and  $\psi_D^-(x)$ , respectively, then each one satisfies the equation:

$$-(\psi_D^\pm)''(x) + (W^2(x) \pm W'(x) - \mu) \psi_D^\pm(x) = 0 \quad (3.33)$$

where

$$W(x) = \frac{\varepsilon\alpha + k}{\sqrt{1 - \alpha^2}} + \sqrt{1 - \alpha^2} \mathcal{A}(x), \quad \mu = \frac{(\varepsilon + \alpha k)^2}{1 - \alpha^2}, \quad (3.34)$$

or

$$W(x) = \frac{\varepsilon \sin \gamma + k}{\cos \gamma} + \cos \gamma \mathcal{A}(x), \quad \mu = \frac{(\varepsilon + k \sin \gamma)^2}{\cos^2 \gamma} \quad (3.35)$$

All this means that the components  $\psi_{D\pm}$  are supersymmetric components of two partner Hamiltonians [12].

These formulas are valid for the magnetic case where  $0 < |\alpha| < 1$ ; however they can be extended to the electric case with  $|\alpha| > 1$ , just by including some pure imaginary terms in (3.34):

$$\sqrt{1 - \alpha^2} = i\sqrt{\alpha^2 - 1}, \quad \alpha = \cosh \gamma$$

For this case if we choose  $\mathcal{A}(x) = \beta x$  then we obtain the effective potential of the harmonic oscillator. This kind of examples were dealt with in Refs. [26, 27].

## 4 Conclusions

In this paper we have investigated the conditions to obtain analytic solutions of Dirac-Weyl equation in graphene under electric and magnetic fields. We have obtained a classification in three cases, which was implicit in many references, but we hope that our approach includes many of them in a simple and general way.

An example, for a pure electric potential, has been examined in detail, where we found some interesting properties such as: i) the relation of this problem with complex effective Schrödinger potentials; ii) the components of the spinor satisfy the formalism of supersymmetric quantum mechanics but with complex superpotentials; iii) the spectrum and bound states have been computed; the effective Hamiltonian is PT symmetric and we show that the eigenfunctions implement this symmetry. Therefore, the PT symmetry is not broken which leads to a real spectrum. The eigenfunctions constitute an orthogonal system.

All these properties are quite appealing, specially the connection of electric potentials with complex effective Schrödinger equations. We have also shown different plots of energy-depth of the potential well, energy-momentum  $k$  of the particle in the  $y$  direction. These two kinds of energy plots are complementary, but they are seldom present in the literature.

We also plotted the form of some eigenfunctions together with the probability and current densities which we expect will enlighten some points of the presentation, in particular, their symmetry properties.

## Acknowledgments

We appreciate the support of the QCAYLE project, funded by the European Union–NextGenerationEU, and PID2020-113406GB-I0 project funded by the MCIN of Spain. Ş. K. thanks Ankara University and the warm hospitality of the Department of Theoretical Physics of the University of Valladolid, where part of this work has been carried out, and to the support of its GIR of Mathematical Physics.

## References

- [1] M. I. Katsnelson, K. S. Novoselov, A. K. Geim, Chiral tunneling and the Klein paradox in graphene, *Nat. Phys.* **2**, 620-625 (2006).
- [2] A. H. C. Neto, F. Guinea, N. M. R. Peres, K. S. Novoselov, A. K. Geim, The electronic properties of graphene, *Rev. Mod. Phys.* **81**, 109-163 (2009).
- [3] M. O. Goerbig, Electronic properties of graphene in a strong magnetic field, *Reviews of Modern Physics* **83**, 1193–1243 (2011).
- [4] C. A. Downing, D. A. Stone and M. E. Portnoi, Zero-energy states in graphene quantum dots and rings, *Phys. Rev.* **84**, 155437 (2011).
- [5] F. Afshari, M. Ghaffarian, Electronic properties of zigzag and armchair graphene nanoribbons in the external electric and magnetic fields, *Physica E Low Dimens. Syst. Nanostruct.* **89**, 86-92 (2017).
- [6] T. H. Do, P. H. Shih, G. Gumbs, D. Huang, Influence of electric and magnetic fields and  $\sigma$ -edge bands on the electronic and optical spectra of graphene nanoribbons, *Phys. Rev. B* **103**, 115408 (2021).
- [7] N. M. Freitag, L. A. Chizhova, P. Nemes-Incze, C. R. Woods, R. V. Gorbachev, Y. Cao, A. K. Geim, K. S. Novoselov, J. Burgdrfer, F. Libisch and M. Morgentern, Electrostatically confined monolayer graphene quantum dots with orbital and valley, *Nano Lett.* **16**, 5798-5805 (2016).
- [8] J. Mao, Y. Jiang, D. Moldovan, G. Li, K. Watanabe, T. Ramezani Masir, F. M. Peeters, E. Y. Andrei, Realization of a tunable artificial atom at a supercritically charged vacancy in graphene, *Nat. Phys.* **12**, 545-550 (2016).
- [9] P. Hewageegana, A. Apalkov, Electron localization in graphene quantum dots, *Phys. Rev. B* **77**, 245426 (2008).
- [10] C. W. J. Beenakker, Andreev reflection and Klein tunneling in graphene, *Rev. Mod. Phys.* **80**, 1337 (2008).
- [11] E. Milpas, M. Torres, G. Murguia, Magnetic field barriers in graphene: an analytically solvable models, *J. Phys.: Condens. Matter* **23**, 245304 (2011).
- [12] Ş. Kuru, J. Negro and L.M. Nieto, Exact analytic solutions for a Dirac electron moving in graphene under magnetic fields , *J. Phys.: Condens. Matter* **21**, 455305 (2009).
- [13] V. Jakubský, Ş. Kuru, J. Negro and S. Tristao, Supersymmetry in spherical molecules and fullerenes under perpendicular magnetic fields, *J. Phys.: Condens. Matter* **25**, 165301 (2013).
- [14] Ş. Kuru, J. Negro and L. Sourrouille, Confinement of Dirac electrons in graphene magnetic quantum dots, *J. Phys.: Condens. Matter* **30**, 365502 (2018).
- [15] D. Demir Kızıllırmak, Ş. Kuru and N. Negro, Dirac-Weyl equations on a hyperbolic graphene surface under magnetic field, *Physica E Low Dimens. Syst. Nanostruct.* **118**, 113926 (2020).
- [16] D. Moldovan, M. Ramezani Masir and F. M. Peeters, Magnetic field dependence of the atomic collapse state in graphene, *2D Materials* **5**, 01501 (2018).
- [17] R. Van Pottelberge, D. Moldovan, S. P. Milovanovic, F. M. Peeters, Molecular collapse in monolayer graphene, *2D Materials* **6**, 045047 (2019).

- [18] D.-N. Le, A.-L. Phan, V.-H. Le, P. Roy, Spherical fullerene molecules under the influence of electric and magnetic fields, *Physica E Low-Dimens. Syst. Nanostruct.* **107**, 60-66 (2019).
- [19] J. H. Bardarson, M. Titov and P. W. Brouwer, Electrostatic confinement of electrons in an integrable graphene quantum dot, *Phys. Rev. Lett.* **102**, 620-625 (2009).
- [20] J. Wang, R. Van Pottelberge, A. Jacobs, B. Van Duppen, F. M. Peeters, Confinement and edge effects on atomic collapse in graphene nanoribbons, *Phys. Rev. B* **103**, 035426 (2021).
- [21] Ş. Kuru, N. Negro, L. M. Nieto and L. Sourrouille, Massive and Massless two- dimensional Dirac particles in electric quantum dot, *Physica E Low Dimens. Syst. Nanostruct.* **142**, 115312 (2022).
- [22] V. Jakubský, Ş. Kuru and N. Negro, Dirac fermions in armchair graphene nanoribbons trapped by electric quantum dots, *Phys. Rev. B* **105**, 165404 (2022).
- [23] A. Contreras-Astorga, F. Correa, and V. Jakubský, Super-Klein tunneling of Dirac fermions through electrostatic gratings in graphene, *Phys. Rev. B* **102**, 115429 (2020).
- [24] C. A. Downing and M. E. Portnoi, Zero-energy vortices in Dirac materials, *Phys. Status Solidi B* **256**, 1800584 (2019).
- [25] R. R. Hartmann and M. E. Portnoi, Two-dimensional Dirac particles in a Pöchl-Teller waveguide, *Scientific Rep.* **7**, 11599 (2017).
- [26] V. Lukose, R. Shankar, and G. Baskaran, Novel electric field effects on Landau levels in graphene, *Phys. Rev. Lett.* **98**, 116802 (2007).
- [27] D.-N. Le, V.-H. Le, P. Roy, Graphene under uniaxial inhomogeneous strain and an external electric field: Landau levels, electronic, magnetic and optical properties, *Eur. Phys. J.* **93**, 158 (2020).
- [28] P. Ghosh, P. Roy, G, Bound states in graphene via Fermi velocity modulation, *Eur. Phys. J.* **132**, 1 (2017).
- [29] F. Guinea, M.I. Katsnelson, A.K. Geim, Energy gaps and a zero-field quantum Hall effect in graphene by strain engineering, *Nat. Phys.* **6**, 30 (2010).
- [30] N. Levy, S.A. Burke, K.L. Meaker, M. Panlasigui, A. Zettl, F. Guinea, A.H. Castro Neto, M.F. Crommie, Strain-induced pseudo-magnetic fields greater than 300 tesla in graphene nanobubbles, *Science* **329**, 544-547 (2010).
- [31] F. Cooper, A. Khare and U. Sukhatme, Supersymmetry and quantum mechanics, *Phys. Rep.* **251**, 267-385 (1995).
- [32] D. J. Fernández C., Supersymmetric quantum mechanics, *AIP Conference Proceedings* **1287**, 3 (2010).
- [33] M. Castillo-Celeita and D. J. Fernandez C., Dirac electron in graphene with magnetic fields arising from first order intertwining operators, *J. Phys. A: Math. Theor.* **53**, 035302 (2020).
- [34] M. Castillo-Celeita, A. Contreras-Astorga and D. J. Fernandez C., Complex supersymmetry in graphene, arXiv: 2203.08173 (2022).
- [35] A. Schulze-Halberg, A. M. Ishkhanyan, Darboux partners of Heun-class potentials for the two-dimensional massless Dirac equation, *Ann. Phys.* **421**, 168273 (2020).

- [36] C. M. Bender and S. Boettcher, Real spectra in non-Hermitian Hamiltonians having PT symmetry, *Phys. Rev. Lett.* **80**, 5243 (1998).
- [37] O. Rosas-Ortiz, O. Castaños and D.Schuch, New supersymmetry generated complex potentials with real spectra, *J. Phys. A: Math. Theor.* **48**, 445302 (2015).
- [38] C.-L. Ho and P. Roy, On zero energy states in graphene, *EPL* **108**, 20004 (2014).
- [39] A. V. Shytov, M. I. Katsnelson, and L. S. Levitov, Atomic collapse and quasi-Rydberg states in graphene, *Phys. Rev. Lett.* **99**, 246802 (2007).
- [40] D. Moldovan, F. M. Peeters, *Nanomaterials for Security*, Springer (2016), pp 3-17.